Biasing Technique of MOSFET for an Accurate and Real-Time-Readout Radiation Sensor

CHOOYAT Pongpisit*
LATHAI Adul*
GE Qi-Wei**
SA-NGIAMSAK Chiranut*†

(Abstract)

This work reports a biasing technique of MOSFET for an accurate and real-time readout radiation measurement particularly during a radiation therapy given to cancer-related patients. The radiation beam energy induces a variation of threshold voltage (V_{TH}) of MOSFET during being exposed to gamma radiation. V_{TH} measurement of five different types of MOSFET were carried out in three methods by using OrCAD and MATLAB. The simulation results conclude that Method III is the most suitable one with high accuracy and ability to read out signal in real time process. Further use of this work is a prototype of a real- time readout radiation measurement using MOSFETs with low cost and high accuracy for patients diagnosed with cancer.

Keywords: MOSFET, Biasing Technique, Current Mode, Radiation, Threshold Voltage, Readout, Real Time

1. Introduction

Radiotherapy is an essential treatment for cancer patients. An inaccurate dose of energy can lead to some side effects such as skin damage, hair loss, fatigue, cardiac and even fibroblast growth [1][2][3]. Thus, an accurate and real-time-readout radiation sensor is cruitial.

Nowadays, there are several types of radiation sensors such as thermoluminescent crystals, ionization chambers, diodes and metal-oxide-semiconductor field effect transistors (MOSFETs) [4][5]. P-channel MOSFETs (p-MOSFETs) have gained numerous attentions as a commercial sensor for radiotherapy due to its advantages on non-destructive and real-time readout, memorizing dose, acceptable sensitivity, simply calibration and low cost [6][7][8].

The fundamental of MOSFET sensing the radiation dose is based on a dependency of the threshold voltage (V_{TH}) of MOSFET on radiation energy. Radiation excites the electron-hole

*Faculty of Engineering, Khon Kaen University, Thailand
**Faculty of Education, Yamaguchi University, Japan
E-mail: † chiranut@kku.ac.th (Corresponding Author)

Journal of East Asian Studies, No.16, 2018.3. (pp.175-183)

pairs in the oxide under the gate layer. The increment of electron-hole pairs causes the shifting threshold voltage. The proper structure of MOSFET suitable for radiation sensors requires a thick oxide layer in order to have higher sensitivity and also linearity [9][10].

Reliability of the readout V_{TH} reflecting the radiation dose depends on its accuracy. There have been several configurations and biasing techniques to achieve this figure of merit. A simple and elegant method of biasing MOSFET with a constant current source was proposed [11]; however, the issue of a proper level of current biasing for different type of MOSFETs has not been investigated, due to the variation of threshold voltage of each commercial MOSFETs may require a different level of biasing current. The objective of this work reports a proper biasing technique of MOSFET applied as an accurate and real-time readout radiation sensor.

2. MOSFET Threshold Voltage Shift

Electric charges inside the MOSFET follows Eq. (1):

$$Q_G + Q_{ox} + Q_C = 0 \qquad (1)$$

where

Q_G is the charge on the gate layer

Q_{ox} is the effective interface charge

Q_C is the charge in the semiconductor under the oxide

With the external voltage V_{GB} applied to the gate-body terminals, the potential distribution and charges distribution of MOSFET are shown in Figure 1.

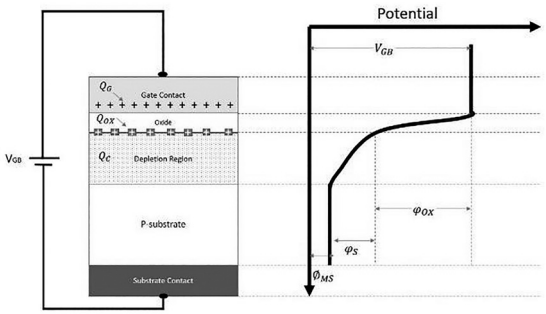

Figure 1. Charges and potential distribution of MOSFET considering 2 terminals model

The effective interface charge, Q_{ox}, is composed of interface trapped charge (Q_{it}), fixed oxide charge, oxide trapped charge (Q_{ot}) and mobile oxide charge.

The exposure of MOSFET to radiation generates the increment of electrical charges in the interface trapped charge (Q_{it}) and the gate oxide trapped charge (Q_{ot}), due to the electron-hole pair generation in the oxide layer [12][13]. The change of both charges cause the shifting of threshold voltage, ΔV_{TH} as shown in Eq.(2) and Eq.(3).

$$V_{TH}=V_{TH0}+\Delta V_{TH} \tag{2}$$

$$\Delta V_{TH}=\frac{\Delta Q_{ot}+\Delta Q_{it}}{C_{OX}}=\frac{t_{ox}}{\varepsilon_{ox}}(\Delta Q_{ot}+\Delta Q_{it}) \tag{3}$$

where

C_{OX} is the oxide capacitance per area unit

V_{TH0} is the threshold voltage before exposure

ΔV_{TH} is the shifted threshold voltage after exposure

The shifted threshold voltage (ΔV_{TH}) is a function of both oxide trapped charge and interface trapped charge which depending on the high-energy ionizing irradiation during radiotherapy; thus ΔV_{TH} can measure the gamma radiation.

3. Materials and Methods

There are several threshold voltage extraction methods in a linear region of transfer IV characteristic such as constant-current, match-point, linear extrapolation, second-derivative, third-derivative, current-to-square-root-of-the-transconductance ratio [14]. This work selected the linear extrapolation as our Method I due to its simplicity and the second-derivative or transconductance (g_m) extrapolation as our Method II due to its most popularity. Finally Method III: constant low current source circuit due to its ability for real-time readout [15].

The accuracy of voltage threshold extraction of Method I-III was carried out by using MATLAB R2013 for Method I-II and OrCAD 16.6 for Method III. The verification was conducted on five commercial p-MOSFETs. The IV Characteristics of those five commercial p-MOSFETs were generated by using OrCAD PSpice with their SPICE models; and the threshold voltage extraction of Method I and II were calculated from the simulated IV characteristic data set using MATLAB as shown in Figure 2 and Figure 3 while the threshold voltage real-time readout of Method III was done by using OrCAD Capture as shown in Figure 4.

Method I and II Procedure:

1. OrCAD PSpice generated IV characteristic data set in text file.
2. MATLAB imported the file and calculated the maximum slope point on the IV characteristic.
3. MATLAB generated the second-derivative data (transconductance, gm) of the imported text file 1 and then calculated the maximum slope point of the the second-derivative data. (this step is only for Method II)
4. Generate the linear equation based on 2 (Method I) or 3 (Method II).
5. Extrapolating the linear equation to calculate the extracted threshold voltage.
6. The reference threshold voltage is obtained from the SPICE model of those five p-MOSFETs

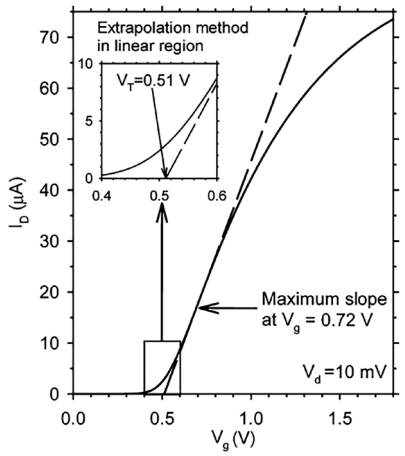

Figure 2 Method I: Extrapolation in Linear Region [14]

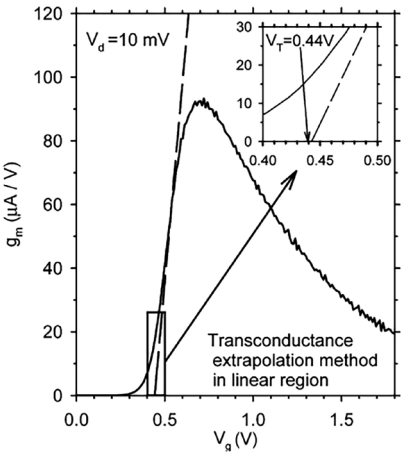

Figure 3 Method II: Transconductance Extrapolation [14]

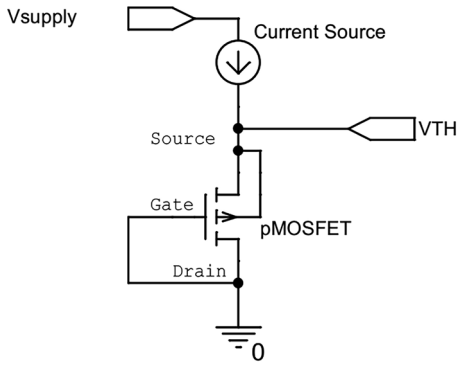

Figure 4 Method III: Real time threshold voltage readout circuit with a low current source

Method III Procedure:

1. Composed the circuit configuration shown in Figure 4 with OrCAD Capture using SPICE model of those five p-MOSFETs.
2. Biasing p-MOSFET under saturation region (V_{SD}>($V_{SG}-|V_{TH}|$)) with a small drain current
3. ** Sweeping the range of current source in order to find the suitable range of current biasing for each p-MOSFET **
4. Set the value of a small drain current source within the range obtained in Step 3 and read the value of V_{SD} which is approximately close to V_{TH} due to the drain current in saturation region is given by Eq.(4)

$$i_D = K_p\,(V_{SG}-|V_{TH}|)^2 \tag{4}$$

$$V_{SG} = \sqrt{\frac{i_D}{K_p}} + |V_{TH}|$$

$$V_{SG} = V_{SD} \cong |V_{TH}| \text{ with small } i_D \tag{5}$$

Where i_D is the drain current, K_p is a constant ($\frac{1}{2}\,\mu_p\,c_{OX}\frac{W}{L}$) and V_{SG} is the source-gate voltage

5. Comparing the readout voltage with the reference threshold voltage obtained from the SPICE model of those five p-MOSFETs.

The simulation of Method III were conducted on OrCAD; and the additional investigation on the different level of the SPICE model of each p-MOSFETs were also studied. The simulation with three different levels (Level 1, Level 3, Level 7) of p-MOSFETs were carried out on the same sheet of schematic using a current mirror to control the level of proper biasing current of each type of p-MOSFETs as shown in Figure 5.

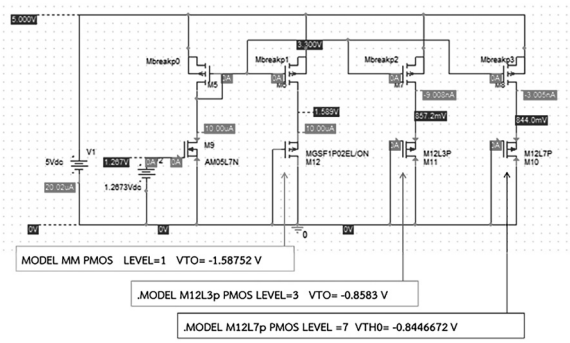

Figure 5. Real time threshold voltage readout circuit with a low current source and current mirror for 3 levels of pMOSFET models

The proper level of current biasing were obtained from Step 3 of Method III Procedure. The level of current were controlled by using current mirror with different width/length (W/L) ratio of MOSFETs.

4. Results and Discussions

The deviation of the extracted threshold voltage with the reference threshold voltage of 5 different type of p-MOSFETs using Method I and II were listed on Table I and II respectively.

Table I: Error Table of Method I:

p-MOS	Reference Vth	Extracted Vth	Error (%)
1st	1.5680	1.5730	0.3182
2nd	1.7652	1.7702	0.2832
3rd	1.8690	1.8740	0.2664
4th	2.0421	2.0471	0.2434
5th	3.3800	3.3849	0.1450

Table II: Error Table of Method II:

p-MOS	Reference Vth	Extracted Vth	Error (%)
1st	1.5680	1.5700	0.1269
2nd	1.7652	1.7680	0.1586
3rd	1.8690	1.8710	0.1059
4th	2.0421	2.0450	0.1405
5th	3.3800	3.3820	0.0592

The error of both methods are rather insignificant; nevertheless, the results on Table I and II clearly show the second-derivative or transconductance (gm) extrapolation provides less error than that of Method I. However, both methods are suitable for the threshold extraction of the unknown SPICE parameters of MOSFETs by using the transfer IV characteristic through the real measurements. Both methods cannot extract the threshold voltage in real-time. Method III offers this function. Table III displayed the value of real-time readout threshold voltage of p-MOSFETs with 3 different levels of SPICE model. Moreover, Method III with our proposed proper biasing technique by sweeping the level of current source in order to allocate the suitable range of current source which controlling by using the current mirror as shown in Figure 5 and its results in Table III clearly display the superior of Method III with even lower error than Method I and II for three levels of SPICE model.

Table III: Error Table of Method III:

p-MOS Level	Reference Vth	Real-time Readout Vth	Error (%)
1	1.5875	1.5890	0.093
3	0.8583	0.8572	0.128
7	0.8446	0.8440	0.079

Further simulation of Method III that can verify its superiority in a real-time readout threshold voltage during radiation energy exposure causing the voltage shifting can be explained below.

The threshold voltage of MOSFET is governed by Eq.(6).

$$V_{TH} = V_{TH0} + \gamma\sqrt{2\phi + V_{SB}} - \gamma\sqrt{2\phi} \quad (6)$$

Where V_{TH0} is the threshold voltage without the substrate biasing (V_{SB} = 0), γ is the body effect (substrate-bias) coefficient, V_{SB} is the source-body voltage. The change in V_{SB} can cause the shifting of the threshold voltage (ΔV_{TH}) . This function was used to demonstrate the ability to apply p-MOSFET as a real-time sensor for radiotherapy as shown in Figure 6.

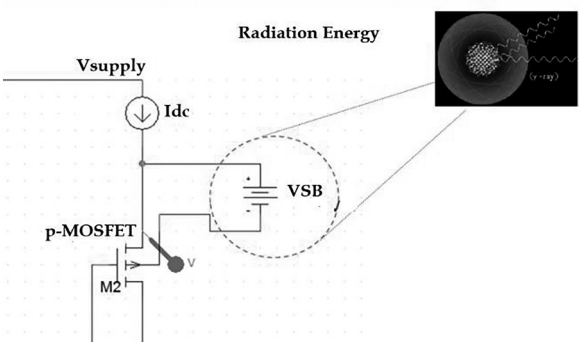

Figure 6. Simulation of the shifted threshold voltage (ΔV_{TH}) due to the external radiation energy by using V_{SB}

V_{SB} was swept from -0.25 volt to +0.25 volt in order to imitate the change of threshold voltage due to the radiation energy exposure; and the readout threshold voltage of p-MOSFET were monitored and plotted in Figure 7. The change of threshold voltage based on the theory governed by Eq.(6) was the reference. The results in Figure 7 show a good agreement between the readout threshold voltage using Method III and the theory.

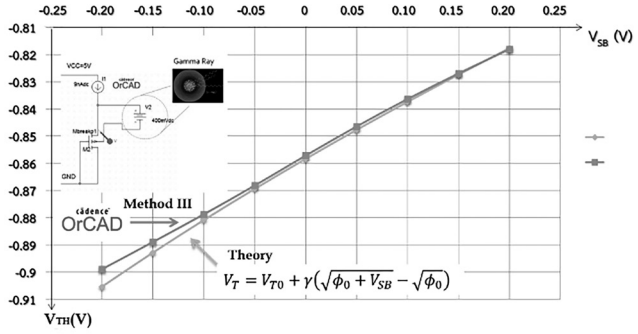

Figure 7. Readout threshold voltage using Method III vs Theory

5. Conclusions

Method I and II are based on IV characteristics of MOSFET. These 2 methods are suitable for the unknown threshold MOSFET such as SPICE parameter device extraction. The results of method I and method II are suitable for pinpointing the V_{TH} reference. However, these two methods are not capable of reading threshold voltage shift due to the gamma radiation during the treatment process in real-time. Method III has been proved its suitability and high accuracy for this application to read out signal in real time process; however, a proper level of biasing current can clearly improve the accuracy of readout threshold voltage using Method III. The combination of our proposed biasing technique with Method III can enhance the existing circuit. Moreover, the demonstration of the ability of Method III to detect the changes of threshold voltage due to the radiation energy exposure that imitated by ΔV_{SB} is also displayed. This proposed circuit can track the change of threshold voltage very well comparing with the theory. Further use of this work is to develop a prototype of the real time read-out gamma-radiation measurement with low cost and high accuracy for patients diagnosed with cancer.

References

[1] N. Alessio, S. Capasso, G. Di, S. Cappabianca, F. Casale, and A. Calarco, "Mesenchymal stromal cells having inactivated RB1 survive following low irradiation and accumulate damaged DNA : Hints for side effects following radiotherapy," *Cell Cycle*, vol. 16, no. 3, pp. 251-258, 2017.

[2] T. Gryc *et al.*, "Idelalisib may have the potential to increase radiotherapy side effects," pp. 1-8, 2017.

[3] C. W. Taylor and A. M. Kirby, "Cardiac Side-effects From Breast Cancer Radiotherapy Statement of Search Strategies Used and Sources of Information Relevance to Radiotherapy Practice," *Clin. Oncol.*, vol. 27, no. 11, pp. 621-629, 2015.

[4] G. E. Knoll and J. Wiley, *Radiation Detection and Measurement Third Edition*, 3rd ed. John Wiley & Sons, 2000.

[5] T. P. M. And and P. V. Dressendorfer, *Ionizing Radiation Effects in MOS Devices and Circuits*. New York: John Wiley & Sons, 1989.

[6] M. N. Amin, R. Heaton, B. Norrlinger, and M. K. Islam, "Small field electron beam dosimetry using MOSFET detector," *J. Appl. Clin. Med. Phys.*, vol. 12, no. 1, pp. 50-57, 2011.

[7] R. A. Price, C. Benson, M. J. Joyce, and K. Rodgers, "Development of a RadFET linear array for intracavitary in vivo dosimetry during external beam radiotherapy and brachytherapy," *IEEE Trans. Nucl. Sci.*, vol. 51, no. 4 I, pp. 1420-1426, 2004.

[8] C. A. K. .C. Hughes, D. Huffman, J.V. Snelling, T.E. Zipperian, A.J. Ricco, "Miniature radiation dosimeter for in vivo radiation measurements," *Int. J. Radiat. Oncol. Biol. Phys.*, vol. 14, no. December 1987, pp. 963-967, 1988.

[9] E. J. Bloemen-van Gurp, A. W. H. Minken, B. J. Mijnheer, C. J. G. Dehing-Oberye, and P. Lambin, "Clinical implementation of MOSFET detectors for dosimetry in electron beams," *Radiother. Oncol.*, vol. 80, no. 3, pp. 288-295, 2006.

[10] I. A.-S. and A. G. R Edgecock, J Matheson, M Weber, E Giulio Villani, R Bose, A Khan, D R Smith, "Evaluation of commercial programmable floating gate devices as radiation dosimeters," *J. Instrum.*, vol. 4, 2009.

[11] N. D. Vasović and G. S. Ristić, "A new microcontroller-based RADFET dosimeter reader," *Radiat. Meas.*, vol. 47, no. 4, pp. 272-276, 2012.

[12] A. Dasgupta, D. M. Fleetwood, R. a Reed, R. a Weller, M. H. Mendenhall, and B. D. Sierawski, "Dose Enhancement and Reduction in SiO2 and High- k MOS Insulators," *IEEE Trans. Nucl. Sci.*, vol. 57, no. 6, pp. 3463-3469, 2010.

[13] J. R. Schwank et al., "Radiation effects in MOS oxides," *IEEE Trans. Nucl. Sci.*, vol. 55, no. 4, pp. 1833-1853, 2008.

[14] A. Ortiz-Conde, F. J. García-Sánchez, J. Muci, A. Terán Barrios, J. J. Liou, and C. S. Ho, "Revisiting MOSFET threshold voltage extraction methods," *Microelectron. Reliab.*, vol. 53, no. 1, pp. 90-104, 2013.

[15] M. S. Martínez-García, F. Simancas, A. J. Palma, A. M. Lallena, J. Banqueri, and M. A. Carvajal, "General purpose MOSFETs for the dosimetry of electron beams used in intra-operative radiotherapy," *Sensors Actuators, A Phys.*, vol. 210, pp. 175-181, 2014.